Abstract No: A-132

FIRST *IN SITU* MEASUREMENTS OF TROPICAL PEATLAND FIRE EMISSIONS: NEW EMISSION FACTORS FOR GREENHOUSE GAS REPORTING AND HAZE FORECASTING

Thomas E L Smith[1*], Catherine M Yule[2], Stephanie Evers[3], Clare Paton-Walsh[4], and Jing Ye Gan[2]

[1]*King's College London, Department of Geography, UK*
[2]*Monash University Malaysia, School of Science, Malaysia*
[3]*University of Nottingham Malaysia Campus, School of Biosciences, Malaysia*
[4]*University of Wollongong, School of Chemistry, Australia*

**Corresponding author: thomas.smith@kcl.ac.uk*

INTRODUCTION

Tropical peat swamp fires in Southeast Asia are a major source of greenhouse gases (GHGs), responsible for climate change; and reactive gases and aerosols, responsible for poor regional air quality affecting hundreds of millions of people (Table 1). Approximately 90% of seasonal haze in Southeast Asia is due to fires burning on peatlands. Despite such damaging impacts, very little is known about the makeup of peatland fire emissions. Current estimates of total emissions from tropical peatland fires, including the important GHGs CO_2 and CH_4, use emission factors derived from one study where a single peat sample was burned in a laboratory. Here, we present the first emission factors to be measured *in situ* at active peat fires burning on degraded peatlands in southeast Pahang, Peninsula Malaysia.

Between 22 July and 22 August 2015, 232 active fire hotspots were detected by MODIS in a tropical peatland region south of Kuantan, Malaysia (Figure 1). During this fire episode, we embarked on a field campaign to measure gaseous emissions at fires in this region using open-path Fourier transform infrared spectroscopy (OP-FTIR). We successfully deployed at eight fires burning in degraded tropical peat. Spectra of infrared light passing through an open-path (10–40 m) through ground-level smoke released from these fires were collected using an infrared lamp and a field-portable FTIR system (Figure 2). The IR spectra were used to retrieve mole fractions of 14 different gases present within the smoke (including CO_2 and CH_4), and these measurements used to calculate emission factors of the various gases emitted by the burning (Table 2). We discuss possible causes for inter-site variability in emissions, and implications of these emission factors for greenhouse gas accounting and haze forecasting.

Table 1: A selection of gas species emitted by peat combustion; their direct/indirect impacts; and the main control on emissions of each species (Modified Combustion Efficiency, MCE; and peat Nitrogen content).

Major compounds	Direct impacts	Secondary impacts	Main control on emissions
CO_2	Climate change		MCE
CH_4	Climate change	Photochemical smog (haze)	MCE
CO	Ozone formation, illness	Photochemical smog (haze)	MCE
NMHCs (C_2H_2, C_2H_4, C_2H_6)	Illness	Photochemical smog (haze)	MCE
VOCs (CH_3OH, CH_3COOH, HCOOH)	Illness/cancer	Photochemical smog (haze)	MCE
N_2O	Climate change	Ozone depletion	MCE and peat N-content
NO, NO_2	Ozone formation, acid rain	Photochemical smog (haze)	MCE and peat N-content
NH_3, HCN	Illness/cancer	Photochemical smog (haze)	MCE and peat N-content

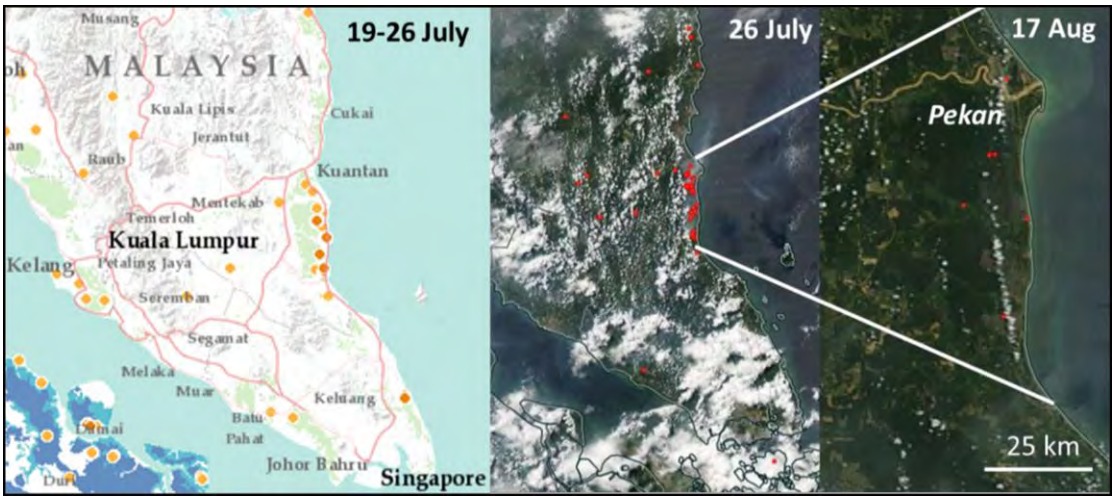

Figure 1: (left) Map of hotspots during the fire outbreak in mid-July (green areas indicate areas of peat), taken from http://fires.globalforestwatch.org/; (centre) MODIS hotpots & visible imagery showing fire hotspots on 26 July 2015 & their associated smoke plume; (right) fire hotspots on 17 August south of Pekan.

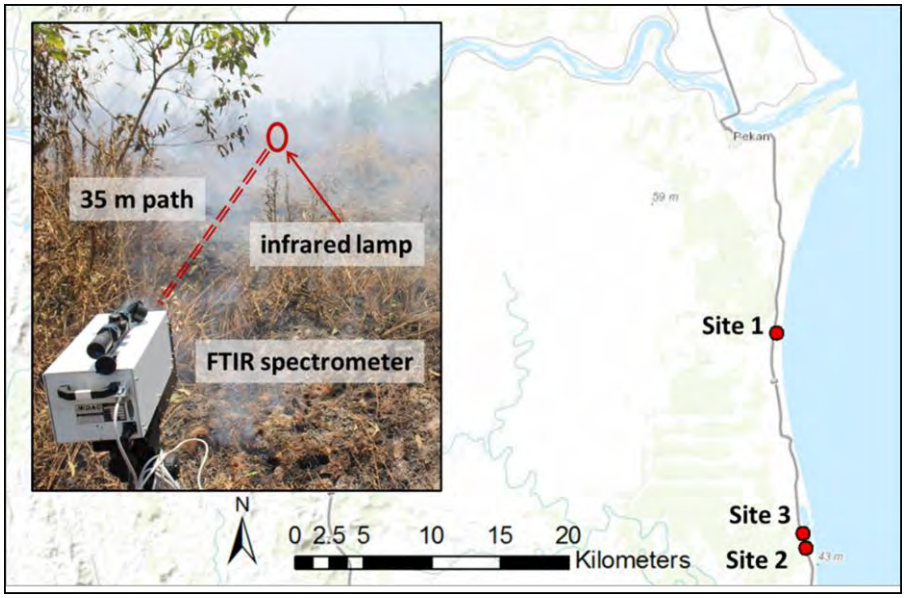

Figure 2: Map with location of three burn sites south of Pekan (see Table 2); (inset) photograph of a typical OP-FTIR setup at Site 2 using a 35 m path between the FTIR spectrometer and infrared lamp.

Table 2: *Site characteristics and results from analysis of peat samples and OP-FTIR-derived MCE for each of the eight burns measured for this paper.*

Burn	Site	Lat (°)	Long (°)	Path (m)	Temp (°C)	Pressure (hPa)	Bulk density (g cm^{-3})	Soil moist (%)	N (%)	C (%)	MCE
P1	1	3.361	103.420	17	34	1008	0.63 ± 0.03	24 ± 0.0	-	-	0.82
P2	1	3.361	103.420	12	36	1011	0.46 ± 0.20	20 ± 1.3	-	-	0.77
P3	2	3.221	103.440	35; 29	40	1008	0.28 ± 0.09	33 ± 0.1	0.69	20.9	0.83
P4	2	3.221	103.440	23; 13	38	1009	0.31 ± 0.10	31 ± 0.1	0.58	18.3	0.79
P5	3	3.231	103.437	20; 12	40	1010	0.25 ± 0.05	41 ± 0.6	1.75	43.3	0.79
P6	2	3.221	103.440	17	40	1010	0.38 ± 0.04	29 ± 1.2	0.51	23.2	0.75
P7	3	3.231	103.437	12; 11; 10	34	1011	0.41 ± 0.11	16 ± 0.3	1.76	41.1	0.78
P8	2	3.221	103.440	11; 11	34	1011	0.37 ± 0.10	28 ± 0.9	1.02	24.3	0.79